A 16,000-yr tephra framework for the Antarctic ice sheet: a contribution from the new Talos Dome core

Biancamaria Narcisi [a,*], Jean Robert Petit [b], Barbara Delmonte [c], Claudio Scarchilli [a], Barbara Stenni [d]

[a] ENEA, C.R. Casaccia, 00123 Roma, Italy
[b] LGGE, CNRS-UJF, Grenoble, France
[c] DISAT, Univ. Studi Milano-Bicocca, Milano, Italy
[d] Department of Mathematics and Geosciences, Univ. Trieste, Trieste, Italy

ABSTRACT

A detailed tephra record for the last 16,000 years of the TALDICE ice core drilled at Talos Dome (East Antarctica, Pacific/Ross Sea sector) is documented. Traces of 26 different explosive volcanic eruptions, dated by ice core chronology and framed within the climate (δ^{18}O) record for the core, have been identified. Glass major element composition and grain size data indicate that all prominent tephra layers derive from Antarctic volcanic activity and likely originated in proximal volcanoes of the Melbourne Volcanic Province (Northern Victoria Land). Two other Antarctic horizons may have originated from the more distant volcanoes of Mount Berlin (Marie Byrd Land, West Antarctica) and Mount Erebus (Ross Island, Southern Victoria Land). Moreover, based on glass-shard geochemistry and a 20-year analysis of atmospheric back trajectories suggesting ash transport from South America to the drilling site by the circumpolar westerly circulation, a few faint microtephra horizons are attributed to Andean volcanic activity. Two of these tephras are interpreted to be related to known Holocene explosive eruptions from the volcanoes of Mount Hudson and Mount Burney. Finally, by comparing compositional features in conjunction with age data, three TALDICE tephras have been successfully correlated with volcanic layers in other ice records of the Antarctic ice sheet. Altogether, our results expand the Antarctic tephrostratigraphic framework and add value to the prospects for continental-scale correlations between ice cores and Southern Hemisphere sediment archives.

© 2012 Elsevier Ltd. All rights reserved.

1. Introduction

In recent decades, tephrochronology has become increasingly important due to its capability to solve issues from disparate disciplines (e.g. Lowe, 2011; and references therein). Tephra layers form isochronous surfaces on a geological timescale. If distinctive in one or more properties and sufficiently widespread, they represent valuable stratigraphic tools for correlation and dating of geological sequences. Among the diverse depositional archives that can potentially contain tephras, polar ice sheets provide unique detailed long records of past climate and atmospheric composition (e.g. Jouzel et al., 2007; Loulergue et al., 2008). Tephra studies of polar ice cores have already proved to be successful in synchronising palaeoclimate signals from widely spaced records (e.g. Davies et al., 2010), in refining timescales obtained by glaciological

modelling (e.g. Narcisi et al., 2006), and in providing complementary information on past atmospheric circulation patterns (e.g. Fiacco et al., 1993).

Tephra investigations of the TALDICE ice core, drilled from the Ross Sea sector of the East Antarctic plateau, offer significant potential for palaeovolcanic and palaeoclimatic reconstructions. This 1620-m long core contains more than 100 volcanic horizons deposited over the past 250,000 years, with average frequency of the visible tephra layers estimated to be one order of magnitude greater than the ones found in deep ice cores from central East Antarctica over the last two glacial cycles. As such, the very rich tephra dossier preserved at TALDICE provides clues on eruption history of nearby volcanoes (Narcisi et al., 2010a). The TALDICE ice core is also a remarkable palaeoclimatic archive, as it holds an uninterrupted record of climate and environmental changes back to Marine Isotope Stage (MIS) 7.5, ~250 ka (Schilt et al., 2010; Stenni et al., 2011). In particular, owing to its relatively high accumulation rate, this core offers a climate record at decadal-scale resolution since the last climatic transition, a period characterised by dramatic and rapid changes throughout the world. TALDICE has been

included in recent comparisons of Antarctic climate records covering the last deglaciation (Stenni et al., 2011) and the present interglacial (Masson-Delmotte et al., 2011) to document past natural variability and time relationship with Northern Hemisphere ice sheet deglacial history, and to identify mechanisms and processes lying behind the observed fluctuations. These studies have shown that, within a general homogeneous pattern, spatial climate variability related to local and regional factors is significant within the Antarctic continent. In this context, further work aimed at inspecting inter-site climate differences could benefit much from tephrochronological investigations. In fact tephra correlations between palaeorecords have several advantageous properties: a) they are independent of climate and can be scattered within the climate record, b) can potentially involve different types of archives geographically spread within the Southern Hemisphere, c) their application for matching is less subjective than the use of volcanic sulphate spikes, that moreover can be recorded only in ice cores, and d) provide time planes circumventing the problem related to the lack of coherent timescales for the compared records.

Despite the fact that several Antarctic tephra records encompassing the last deglaciation and/or the present interglacial (Holocene) have been already presented (e.g. Smellie, 1999; and references therein), to date the potential of continental-scale tephra correlations has not been fully exploited. The best example of a Holocene volcanic marker across Antarctica remains the 3.5-ka tephra from South Sandwich Islands (southern Atlantic Ocean), which was originally identified in Vostok and South Pole ice cores (Palais et al., 1987) and recently detected also in the EPICA-Dome C (hereafter EDC) record (Narcisi et al., 2005). No tephra correlations linking the Antarctic ice with Southern Hemisphere sediment sequences have been presented thus far.

Here, we present the results of a tephra investigation carried out throughout the last deglaciation and Holocene sections of the TALDICE ice core, with the purpose of expanding the Antarctic tephrostratigraphic framework. We provide a detailed tephra inventory for this site including visible and non-visible ash layers. We then propose source attribution and tephra correlations between sequences of the South polar region, based on the comparison of chronological information and major element geochemical data and using particle size characteristics and the results of back trajectory studies as supplementary arguments.

2. Materials and methods

The European TALDICE project (www.taldice.org) was launched to augment scientific knowledge on palaeoclimate changes in near-coastal regions of the Antarctic ice sheet. For this purpose, a 1620-m long ice core was drilled at Talos Dome (72°49′S, 159°11′E; 2315 m), an ice dome on the eastern edge of the East Antarctic Plateau, during the field seasons 2004–2008. Climatological and glaciological characteristics of the drilling site are reported in Frezzotti et al. (2007) and Masson-Delmotte et al. (2011).

In this work we focused on the core section between 73 and 800 m depth, corresponding to the time period ca 560–16,300 years BP (before present, where present is defined as 1950 AD), with an average age uncertainty of about 100 years. The adopted age scale (Severi et al., 2012) represents a refinement of the first official chronology of the Talos Dome core (Buiron et al., 2011) and was obtained by synchronising the TALDICE volcanic sulphate signals to the EDC record with transfer of the timescale presented by Lemieux-Dudon et al. (2010) to the studied core.

In the considered core interval we located a total of 24 volcanic ash horizons related to primary air fall deposition (Table 1 and Fig. 1). Among them, 12 conspicuous tephra layers were identified during core logging/processing. Salient physical and macroscopic

Table 1
Details for the identified tephra-bearing horizons.

Sample	Visible	Bottom depth (m)	Age yr BP[a]	Maximal grain size (μm)	Method for single shard chemical analysis	Suggested source
TD85	x	84.37	670 ± 7	100	WDS	Melbourne
TD87	x	86.20	694 ± 7	80–90	WDS	Melbourne & Mt Berlin
TD193		192.25	2021 ± 66	10	EDS	Mt Hudson
TD210		209.50	2267 ± 59	15	EDS	Melbourne
TD216		215.50	2355 ± 54	<10	EDS	South American – possibly Mt Hudson
TD238	x	237.31	2684 ± 47	80	WDS	Melbourne
TD239	x	238.12	2699 ± 48	100–150	WDS	Melbourne
TD281		280.27	3375 ± 82	80	EDS	Melbourne
TD282		281.50	3392 ± 82	10	EDS	South American – possibly Puyehue-Cordón Caulle
TD299		298.25	3677 ± 92	10	EDS	Mt Burney
TD341		340.25	4420 ± 88	10	EDS	Extra-Antarctic unidentified
TD388-1	x	387.76	5277 ± 49	60	WDS	Melbourne
TD388-2	x	387.77	5277 ± 49	40	WDS	Melbourne
TD504		503.25	7570 ± 144	10	EDS	Melbourne & possibly Mt Erebus
TD554		554.00	8792 ± 193	20	EDS	Melbourne
TD642		641.75	10,900 ± 151	100	EDS	Melbourne
TD655		654.50	11,199 ± 137	15–20	EDS	Extra-Antarctic unidentified
TD662	x	661.86	11,364 ± 132	50	WDS	Melbourne
TD667		666.40	11,476 ± 128	15	EDS	Extra-Antarctic unidentified
TD681	x	680.78	11,820 ± 128	60–80	WDS	Melbourne
TD720	x	719.78	13,010 ± 127	40	WDS	Melbourne
TD741	x	740.34	13,771 ± 131	100–150	WDS	Melbourne
TD779	x	778.07	15,193 ± 145	50–70	WDS	Melbourne
TD783	x	782.59	15,370 ± 150	25	WDS	Melbourne

[a] Age according to Severi et al. (2012), estimated uncertainty from Lemieux-Dudon et al. (2010). BP stands for before 1950 AD.

features of TALDICE visible layers were already illustrated in Narcisi et al. (2010a). The narrow ice samples containing visible tephra layers were sub-sampled for subsequent particulate matter recovery. Moreover, in order to complement the inventory of the prominent tephras, about 30 discrete (25 cm long) ice core samples between 73 and 700 m depth were filtered and examined microscopically for the search of primary volcanic material. These samples, formerly analysed for aeolian dust studies (Albani et al., 2012), showed anomalous features, either as mass concentration or as grain size values, compared to typical continental dust in East Antarctic ice. 12 of the investigated ice intervals proved to contain significant concentrations of glass shards showing unmodified typical morphologies and coherent geochemistry (see the discussion in Section 3). Thus, they were considered to be formed directly from volcanic plumes without significant reworking prior to and during deposition on the ice sheet.

All tephra samples were the subject of quantitative grain size measurements by Coulter Counter (Fig. 2), characterisation of particle morphology and determination of maximum grain size by scanning electron microscope (Fig. 3), and chemical analysis by electron microprobe. Chemical (nine major elements) characterisation was performed only on pristine glass particles. Detrital windblown components, significant in some studied samples bearing invisible tephras, and mineral crystals were avoided using
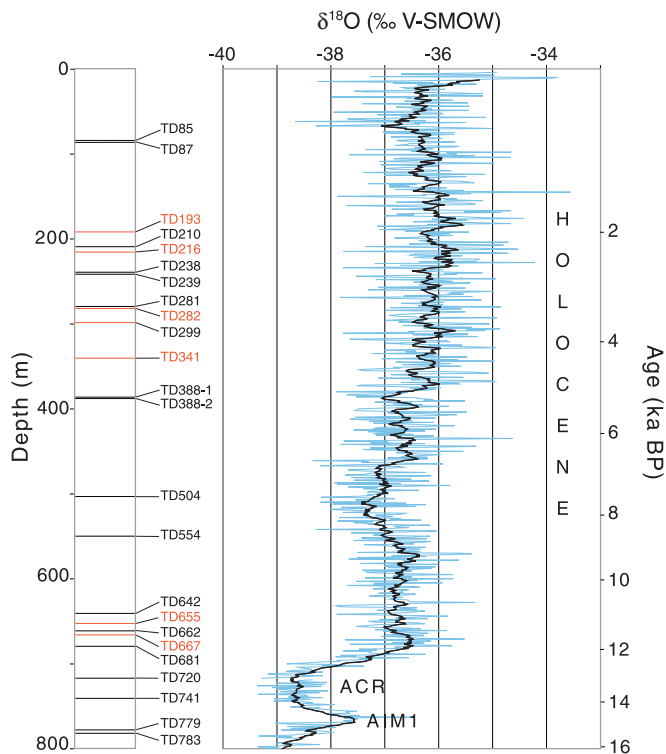
Fig. 1. Stratigraphic position of the tephra horizons identified in the TALDICE ice core plotted alongside the stable isotope ($\delta^{18}O$) profile (Stenni et al., 2011; raw data as thin line, data averaged over 10 m-sections as black line). Although single horizons are represented, two distinct tephra populations were identified in the samples TD87 and TD504. Tephras from extra-Antarctic volcanic sources are indicated in red. AIM1 and ACR climate events are indicated. The ice core timescale is from Severi et al. (2012). (For interpretation of the references to colour in this figure legend, the reader is referred to the web version of this article.)

systematically the electron microscope during the analytical sessions. We used wavelength-dispersive X-ray spectrometry (WDS) for glass fragments that were large enough for embedding and polishing, and energy dispersive X-ray spectrometry (EDS) for very fine grained and/or sparse tephras (e.g. Narcisi et al., 2005). Operating conditions for WDS were as follows: accelerating voltage
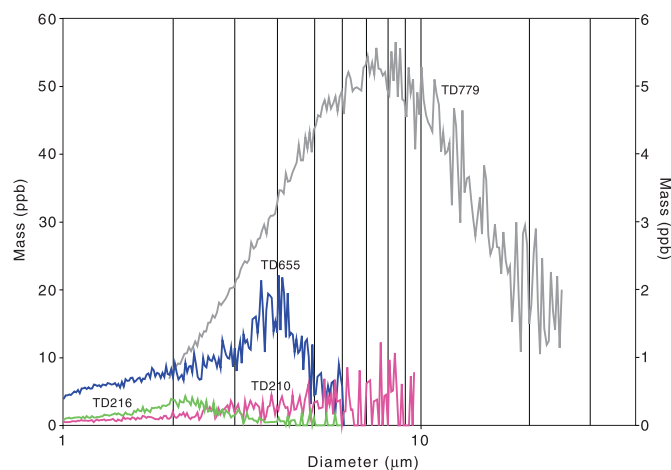
Fig. 2. Mass-size distributions of typical visible and invisible tephras obtained by Coulter counter measurements (description of analytical procedures is reported in Delmonte et al., 2002). Note different scales on ordinate axes (left y axis for TD779, right y axis for the other samples).

20 kV, beam diameter 1 μm, peak counting times and beam current 10 s and 2 nA, respectively for Na, K, Al and Si, and 20 s and 20 nA, respectively for the remaining elements, backgrounds counted for half of the peak-count time. Operating conditions for EDS were as follows: accelerating voltage 25 kV, acquisition time 50 s, X-ray counts $1000-1500\ s^{-1}$. Comparison of EDS and WDS data obtained on the same samples indicated the comparability of results. Reference materials (Morgan and London, 2005; Jochum et al., 2006) were routinely measured to check precision and accuracy of the analyses. Typical analytical errors are ca 1 wt.% relative for SiO_2, 1–2 wt.% relative for Al_2O_3 and 3–5 wt.% relative for the other element oxides. Geochemical results are reported in Tables 2 and 3 and are illustrated in biplots of selected oxides (Figs. 4–6).

3. General features of the tephra samples

Microscopic inspection of the recovered volcanic material indicates that the TALDICE samples are variously graded (Table 1 and Fig. 3). Typically, prominent thick ash layers are rather coarse, with maximum size of a few ten of microns, even up to 150 μm. Conversely, invisible ash horizons are usually very fine grained, with maximum size of the volcanic ash seldom exceeding 15–20 μm. Modes of the grain size distributions obtained from Coulter Counter analysis are also very variable, from 2 to >10 μm (Fig. 2). Ash layers obvious to the naked eye typically show high mass concentration and grain size values. Invisible ash horizons are usually not very concentrated but often show cuspate distribution curves.

Chemical analyses of individual tephra samples were performed on single glass shards. Unlike whole-rock geochemistry, grain-specific analyses adequately fingerprint a tephra deposit and potentially enable detection of compositional variability that can represent a distinctive intrinsic feature of a tephra. The obtained results show that the investigated tephra samples display different degrees of compositional heterogeneity (Tables 2 and 3, and Figs. 5 and 6). Many tephra layers contain a fairly homogeneous single glass population, as testified by tight clustering of data points. By comparison, glass shards in a few horizons (e.g. TD238 and TD299) show a wide compositional range along a fractionation trend. This coherent pattern excludes mixing with unrelated volcanic particles (i.e. windblown dust) and indicates direct fallout from a distinct explosive event generated from a zoned magma chamber. A further case is represented by horizons comprising two or more glass-shard compositions (e.g. TD87 and TD504). Complex glass geochemistry, due to occurrence of mixed populations or outliers, can be due to compositional changes within a single explosive event, or to deposition from simultaneous eruptions originated in different sources.

In Fig. 4 chemical data for the identified tephras are plotted on the K_2O versus SiO_2 classification diagram (Rickwood, 1989; and references therein). Results for homogeneous layers and subpopulations inside single samples are represented as mean and one standard deviation (error bars) from multiple analyses, while for heterogeneous samples we plot individual analytical points. Two main compositional groups can be identified that reflect origin from volcanoes in different geodynamic settings. The largest group, including all visible tephra layers and a few horizons undetectable by the naked eye, has glass compositions belonging to the shoshonite series. Based on the Total Alkali-Silica (TAS) classification (Le Bas et al., 1986), the most represented composition in this alkali-rich group is trachyte (Table 2). Volcanic products with alkaline geochemical affinity typically occur in intraplate tectonic domains. The alkali-rich TALDICE tephra horizons can thus be unambiguously attributed to Antarctic volcanic provinces connected to the West Antarctic Rift System (Wörner, 1999). The second sample
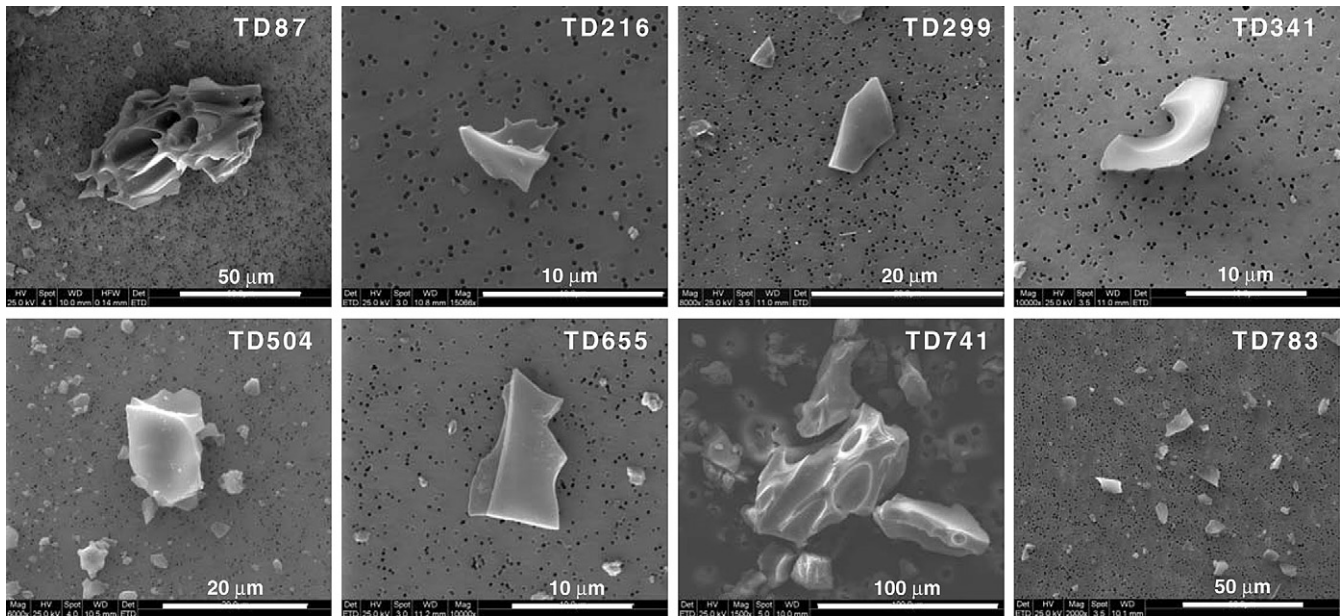
Fig. 3. Scanning electron microscope images of typical glass shards from selected tephra horizons.

group, including only fine-grained volcanic horizons not visible to the naked eye, has tholeiitic to calc-alkaline compositions with sub-alkaline geochemical affinity. According to the TAS classification, samples of this group are mainly dacitic and rhyolitic in composition (Table 3). This geochemical signature is typical of volcanism in subduction tectonic zones. In the Southern Hemisphere, potential source volcanic provinces from a subduction setting are those of southern Andes, South Sandwich Islands (southern Atlantic Ocean), South Shetland Islands (off the Antarctic Peninsula) and New Zealand, all located outside the Antarctic continent. The geochemical signature along with the tiny grain size of the horizons suggesting long-distance transport of ash, indicate that the sub-alkaline tephras detected at TALDICE originated from extra-Antarctic volcanic regions.

4. Sources of TALDICE tephra horizons and correlation between palaeoarchives

We used the geochemical fingerprint of the glass shards combined with physical properties of the pyroclastic material to assess volcanic provenance of the identified tephras. Also, chronological criteria help narrow the set of possible sources and are essential for attribution to specific events known at source volcanoes and/or for correlation with tephra layers occurring in other stratigraphic sequences. Chemical compositions and ice-core related ages of the studied samples were compared with published geochemistries of Quaternary volcanoes in and around Antarctica with the aim of determining the parent volcanoes and perhaps even identify correlative eruptions for the TALDICE tephras. This is a challenging exercise, given the large number of potential source volcanoes under consideration and incomplete inventories of pyroclastic deposits due to the remote location of volcanoes, extensive snow/ice cover and shortage of stratigraphically significant sections. Additionally, we considered Antarctic ice tephra records spanning similar time periods to propose tephra correlation and thus establish precise time linking between geographically separated palaeoarchives. Whenever available in the literature, electron microprobe geochemical results were preferred for comparison, since data obtained using other

techniques could lead to misleading conclusions. Geochemical matches between samples were evaluated using the similarity coefficient (SC) by Borchardt et al. (1972) and including all major elements in the SC calculation. A chemically identical pair would yield a SC of 1. In practice, SC values exceeding the 0.92 minimum threshold indicate positive matching (Froggatt, 1992). When only bulk-sample geochemical data were available in the literature and in cases where the low number of analyses did not allow derivation of reliable averages, chemical similarities were tested through graphical comparison of compositional data.

Description of the most significant tephra layers together with suggested sources and stratigraphic correlations are given below. Graphic comparisons between our individual chemical analyses and published data for relevant volcanic samples are portrayed in Figs. 5 and 6. Based on the above considerations on glass petrological characteristics and related tectonic settings, we subdivided the studied samples into Antarctic and extra-Antarctic tephra layers. Within each geographic group, volcanic layers are presented in order of increasing age.

4.1. Antarctic tephra layers

A discussion on potential sources of prominent TALDICE tephra layers has been already reported by Narcisi et al. (2010a). Mount Melbourne, Mount Rittmann, and The Pleiades (Melbourne Volcanic Province) located ∼250 km from the coring site, are the likely source for the majority of the alkali-rich tephras in the ice core. In addition to geographical closeness and explosive activity of these volcanoes during Quaternary to recent times, geochemical compositions of coarse-grained ash layers identified in the considered core sections closely match compositional range of Melbourne products and rule out other Antarctic volcanoes. Tephras TD87b and TD504a deviate from the bulk of alkaline samples, as their geochemical features are not consistent with derivation from the Melbourne Volcanic Province. As discussed below, they are inferred to derive from other rift volcanic sources within the Antarctic continental plate.

Visible layer **TD87** contains two admixed glass populations, labelled **TD87a** and **TD87b**, respectively (Table 2 and Fig. 5a).

Table 2
Major element composition of glass shards from TALDICE tephra horizons related to Antarctic volcanic activity. Data (in weight percent, wt%) are recalculated to a sum of 100 wt% and are presented as mean and one standard deviation of *n* analyses of different glass shards from a tephra sample. Unaveraged data are presented for heterogeneous horizons and/or outlier glass shards. Original oxide totals before recalculation are also given. Total iron expressed as FeO. TAS (Total Alkali-Silica) classification according to Le Bas et al. (1986).

Sample	n	SiO_2	TiO_2	Al_2O_3	FeO	MnO	MgO	CaO	Na_2O	K_2O	Total	TAS classification
TD85	8	65.64	0.50	15.83	5.51	0.18	0.22	1.85	5.43	4.84	98.59	Trachyte
st. dev.		0.36	0.02	0.52	0.20	0.04	0.03	0.05	0.24	0.12	1.60	
TD87a	6	61.58	0.43	16.74	6.54	0.28	0.15	1.18	7.92	5.17	99.00	Trachyte
st. dev.		0.37	0.06	0.35	0.15	0.05	0.02	0.05	0.40	0.28	0.89	
TD87b	1	57.98	0.58	13.61	12.66	0.68	0.43	2.20	7.25	4.61	97.76	Trachyte
TD87b	1	58.39	0.66	14.07	11.82	0.54	0.42	2.27	7.18	4.65	95.34	Trachyte
TD87b	1	59.76	0.39	14.69	10.03	0.54	0.25	1.75	8.54	4.05	99.41	Trachyte
TD210	10	68.7	0.4	13.2	5.3	0.2	0.2	1.3	6.1	4.8	96.2	Trachyte
st. dev.		0.9	0.2	0.3	0.4	0.1	0.1	0.3	0.8	0.5	1.8	
TD238a	4	49.96	3.59	15.74	11.38	0.22	3.56	8.14	4.77	2.64	96.36	Phonotephrite
st. dev.		0.98	0.18	0.09	0.53	0.03	0.21	0.23	0.52	0.19	2.24	
TD238b	1	53.08	2.92	16.10	9.78	0.19	2.64	5.87	5.77	3.64	97.96	Tephriphonolite
TD238b	1	58.13	1.63	16.99	6.89	0.18	1.69	3.62	5.99	4.86	99.40	Latite
TD238b	1	65.78	0.39	15.67	4.60	0.14	0.21	1.51	6.53	5.16	94.31	Trachyte
TD239	18	47.32	3.88	16.18	10.94	0.22	4.11	10.01	4.59	2.77	97.77	Tephrite
st. dev.		1.28	0.41	0.61	0.84	0.04	0.72	1.37	0.56	0.57	1.30	
TD281	10	64.1	0.4	15.5	5.7	–	0.2	1.0	7.9	5.2	95.9	Trachyte
st. dev		1.1	0.3	0.8	1.0		0.2	0.3	1.4	0.7	1.7	
TD388-1	6	51.30	3.14	14.04	13.68	0.29	2.98	6.87	4.35	3.36	97.91	Shoshonite
st. dev.		1.18	0.08	0.23	0.60	0.03	0.32	0.25	0.36	0.32	1.46	
TD388-2a	18	56.77	1.75	15.06	11.11	0.30	1.71	4.99	4.90	3.41	97.82	Latite
st. dev		0.66	0.11	0.52	0.89	0.04	0.19	0.60	0.46	0.59	1.47	
TD388-2b	1	50.14	3.49	16.10	11.09	0.22	3.89	8.43	4.31	2.36	94.21	Shoshonite
TD388-2b	1	67.43	0.76	13.54	6.05	0.11	0.42	1.89	4.58	5.21	95.77	Trachyte
TD504a	8	58.4	1.0	18.6	4.5	0.5	1.0	1.6	9.6	4.9	96.4	Phonolite
st. dev.		1.9	0.7	1.1	0.9	0.4	0.7	0.8	0.9	0.6	2.0	
TD504b	6	48.9	3.6	16.3	9.8	0.3	5.2	8.2	5.9	1.9	95.6	Phonotephrite
st. dev.		1.7	1.2	1.2	1.5	0.2	0.9	1.4	1.3	0.3	1.9	
TD554	11	63.7	0.2	16.1	5.2	0.3	0.4	0.6	9.6	4.1	95.1	Trachyte
st. dev		1.0	0.1	0.7	0.8	0.2	0.2	0.2	1.0	0.4	2.1	
TD642	12	63.8	0.2	15.4	6.5	0.3	0.3	0.8	8.1	4.8	96.9	Trachyte
st. dev.		0.8	0.2	0.4	0.9	0.2	0.2	0.2	0.7	0.4	1.3	
TD662	6	66.58	0.16	15.91	4.30	0.21	0.09	1.04	6.69	5.02	96.81	Trachyte
st. dev.		1.23	0.06	0.60	1.23	0.07	0.05	0.17	0.46	0.43	1.79	
TD681	14	50.61	2.68	16.83	10.49	0.23	3.55	7.23	5.49	2.89	97.07	Phonotephrite
st. dev.		0.67	0.06	0.43	0.19	0.02	0.23	0.29	0.72	0.24	1.27	
TD720	5	65.53	0.13	16.49	3. 87	0.19	0.02	0.80	8.05	4.93	96.15	Trachyte
st. dev.		0.62	0.05	1.18	1.55	0.09	0.02	0.18	0.67	0.22	1.65	
TD741	11	61.55	0.35	17.50	5.51	0.21	0.15	1.07	8.39	5.27	98.14	Trachyte
st. dev.		0.32	0.01	0.33	0.17	0.02	0.02	0.05	0.56	0.27	1.28	
TD779	18	62.41	0.47	18.03	4.91	0.18	0.28	1.19	7.30	5.25	97.71	Trachyte
st. dev.		0.54	0.01	0.29	0.09	0.02	0.03	0.06	0.50	0.20	0.97	
TD783	10	59.93	0.88	17.69	6.78	0.23	0.91	2.43	6.51	4.64	98.18	Trachyte
st. dev.		1.25	0.14	0.42	1.26	0.06	0.28	0.73	0.47	0.55	1.26	

Trachytic tephra TD87a was already found in a pilot shallow core drilled at Talos Dome in 1996–97, where it was dated at 1254 ± 2 AD (0.7 ka BP) using counting of annual sulphate and nitrate fluctuations and comparison with records of major known volcanic eruptions (Narcisi et al., 2001). This tephra, most probably derived from The Pleiades volcanoes, represents a valuable stratigraphic marker across the Antarctic ice sheet as it correlates to a volcanic horizon in the Taylor Dome and Siple Dome B ice cores (Dunbar et al., 2003), ca 550 and 1500 km, respectively from Talos Dome (Fig. 7). A good geochemical match (SC values of 0.96 and 0.98 for correlative tephras in the Taylor Dome and Siple Dome B ice cores, respectively) supports this correlation. Moreover, according to Dunbar et al. (2010), this tephra was recently identified further away in central West Antarctica in the WAIS Divide ice core. The subordinate set of glass shards (TD87b) is also trachytic in composition (SiO_2 58–60 wt% and Total Alkali 12–12.5 wt%) but with a chemical signature inconsistent with The Pleiades products. This distinct population, which was not detected in any previously studied core, chemically resembles very young (<10.5 ka) tephras emitted by the West Antarctic volcano of Mount Berlin, Marie Byrd Land province (Dunbar et al., 2008) (Fig. 5a). This still thermally active volcano has produced several explosive eruptions in Late Quaternary times and the related widespread ash layers are preserved in the West Antarctic ice sheet (e.g. Wilch et al., 1999) and further away, in deep ice cores from the East Antarctic Plateau (e.g. Narcisi et al., 2010b; and references therein) and in circumpolar glaciomarine sediments (Hillenbrand et al., 2008). Mount Berlin could thus be a suitable source of ash at TALDICE and we suggest that the identified tephra is attributed to an explosive event occurred at this volcano almost eight centuries ago coevally with The Pleiades eruption.

Layers **TD238** (2.68 ka BP) and **TD388-2** (5.28 ka BP) display similar geochemical patterns. Both are characterised by a fairly tight main geochemical population (TD238a and 388-2a, respectively) with outliers (TD238b and 388-2b, respectively) that however appear to follow a coherent fractionation trend (Fig. 5b). Glass composition in both layers closely matches analyses of Mount Melbourne products from the recent volcanic sequence (Wörner et al., 1989). Interestingly, similar continuum of compositions has been found also in the sample SDMA-657 (304 AD, 1.65 ka BP) from the West Antarctic Siple Dome core (Kurbatov et al., 2006), however the different estimated ages rule out the stratigraphic

Table 3
Major element composition of volcanic glass from TALDICE tephra horizons related to extra-Antarctic volcanic activity. Data (in weight percent, wt%) are recalculated to a sum of 100 wt% and are presented as mean and one standard deviation of n analyses of different glass shards from a tephra sample. Unaveraged data are presented for heterogeneous horizons. Original oxide totals before recalculation are also given. Total iron expressed as FeO. TAS (Total Alkali-Silica) classification according to Le Bas et al. (1986).

Sample	n	SiO_2	TiO_2	Al_2O_3	FeO	MnO	MgO	CaO	Na_2O	K_2O	Total	TAS classification
TD193	12	50.6	2.2	16.5	9.9	0.2	6.8	8.2	4.5	1.2	97.0	Trachybasalt
st. dev.		1.0	0.5	0.7	1.2	0.1	1.2	0.9	0.5	0.1	1.3	
TD216	10	69.6	0.9	15.6	2.4	0.6	1.1	1.1	5.5	3.4	95.5	Rhyolite
st. dev.		1.7	0.7	0.9	0.9	0.5	0.7	0.7	0.7	0.5	2.2	
TD282	13	70.5	0.8	13.8	4.4	0.2	1.0	2.3	5.0	2.1	96.7	Dacite
st. dev.		0.5	0.3	0.8	0.4	0.1	0.4	0.5	0.6	0.4	1.5	
TD299	1	66.8	1.1	13.3	5.9	0.1	2.4	3.8	5.6	1.0	95.5	Dacite
TD299	1	67.0	0.8	15.2	4.8	0.1	2.1	3.5	5.1	1.3	96.3	Dacite
TD299	1	67.0	0.9	15.5	5.1	0.4	2.0	3.0	4.9	1.2	95.9	Dacite
TD299	1	67.3	0.8	14.5	5.4	0.2	1.2	4.5	5.2	1.0	97.1	Dacite
TD299	1	68.7	0.4	15.4	4.1	0.2	1.4	3.7	5.1	1.1	95.9	Dacite
TD299	1	71.7	0.2	13.0	4.9	0.2	1.6	2.7	4.7	1.1	94.9	Rhyolite
TD299	1	72.9	0.9	13.8	4.2	0.1	1.8	1.7	3.3	1.4	95.5	Rhyolite
TD299	1	73.4	0.5	13.0	3.7	0.1	1.7	2.6	3.4	1.5	96.0	Rhyolite
TD341	13	77.4	0.2	12.7	0.5	0.4	0.2	0.4	4.7	3.7	95.8	Rhyolite
st. dev.		0.5	0.2	0.4	0.3	0.2	0.2	0.2	0.4	0.2	1.4	
TD655	19	77.4	0.4	12.6	0.8	0.3	0.4	0.6	3.0	4.7	95.4	Rhyolite
st. dev.		0.9	0.2	0.5	0.4	0.2	0.3	0.3	0.6	0.5	2.0	
TD667	21	77.8	0.2	12.3	0.8	0.2	0.2	0.6	3.9	4.1	96.1	Rhyolite
st. dev.		1.0	0.2	0.7	0.3	0.2	0.2	0.4	0.6	0.4	1.8	

equivalence between any of the TALDICE layers with the Siple Dome tephra.

Tephritic tephra **TD239** (2.70 ka BP) from Melbourne volcanic activity was easily identified during core logging because of its dark colour and remarkable thickness (cf. Fig. 3A of Narcisi et al., 2010a). Due to its outstanding macroscopic features it could be obvious also in blue ice fields of the Transantarctic Mountains. Indeed, the ice succession exposed at Frontier Mountain (ca 30 km SE from Talos Dome) contains a few tephritic layers that appear geochemically similar to sample TD239 (Curzio et al., 2008). The published Frontier Mountain tephra record however, includes only the most prominent and best exposed layers and moreover no chronological control is available for the Lateglacial-Holocene ice sections. In spite of these limitations, we confidently correlate TD239 with the Frontier Mountain FMTop-ZC1-ZC1bis tephritic horizon (Fig. 5c), located at the top of the series and appearing as the thickest and

darkest tephra layer of the whole ice field (Curzio et al., 2008). Matching of glass-shard chemistries (SC 0.95) along with similar macroscopic aspect and stratigraphic position support this correlation. Additionally, the TALDICE layer is chemically similar to a coarse tephra outcropping in the Allan Hills blue ice region (Nishio et al., 1985), some 400 km North of Talos Dome (Fig. 5c). However, aside from the chemical similarity (SC 0.96), no secure correlation can be made with the Allan Hills tephra due to the lack of chronostratigraphic information for the blue ice.

Volcanic glass in the very fine-grained invisible tephra horizon **TD504** (7.57 ka BP) shows bimodal composition (Table 2 and Fig. 5d), one featuring phonolite (**TD504a**), and the other phono-tephrite (**TD504b**). Within Quaternary volcanoes connected to the West Antarctic Rift System, phonolitic products are typical of Mount Erebus (Southern Victoria Land, ca 600 km from Talos Dome), an active stratovolcano that has produced a few tens of tephra layers in
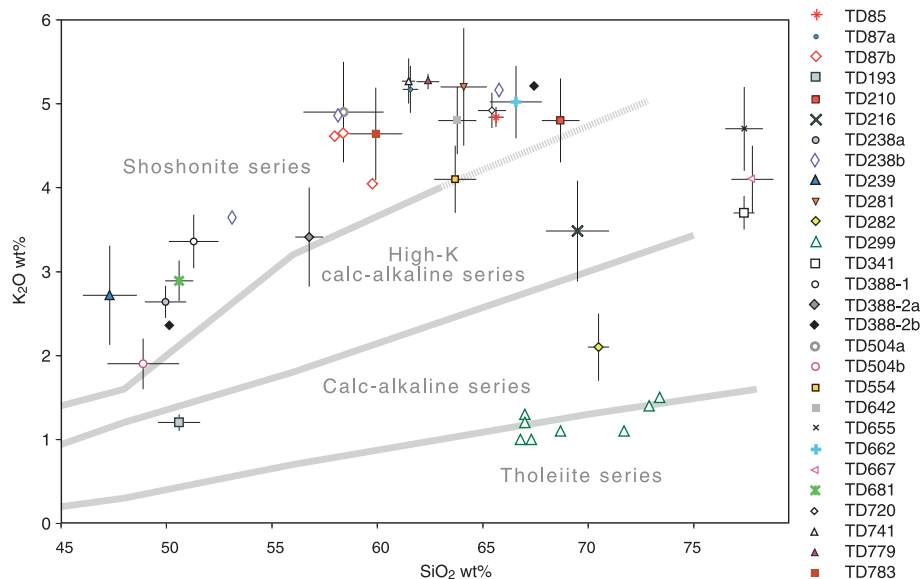
Fig. 4. K_2O versus SiO_2 classification scheme (Rickwood, 1989, and references therein) showing compositions of tephras from the TALDICE ice core. Error bars indicate one standard deviation.
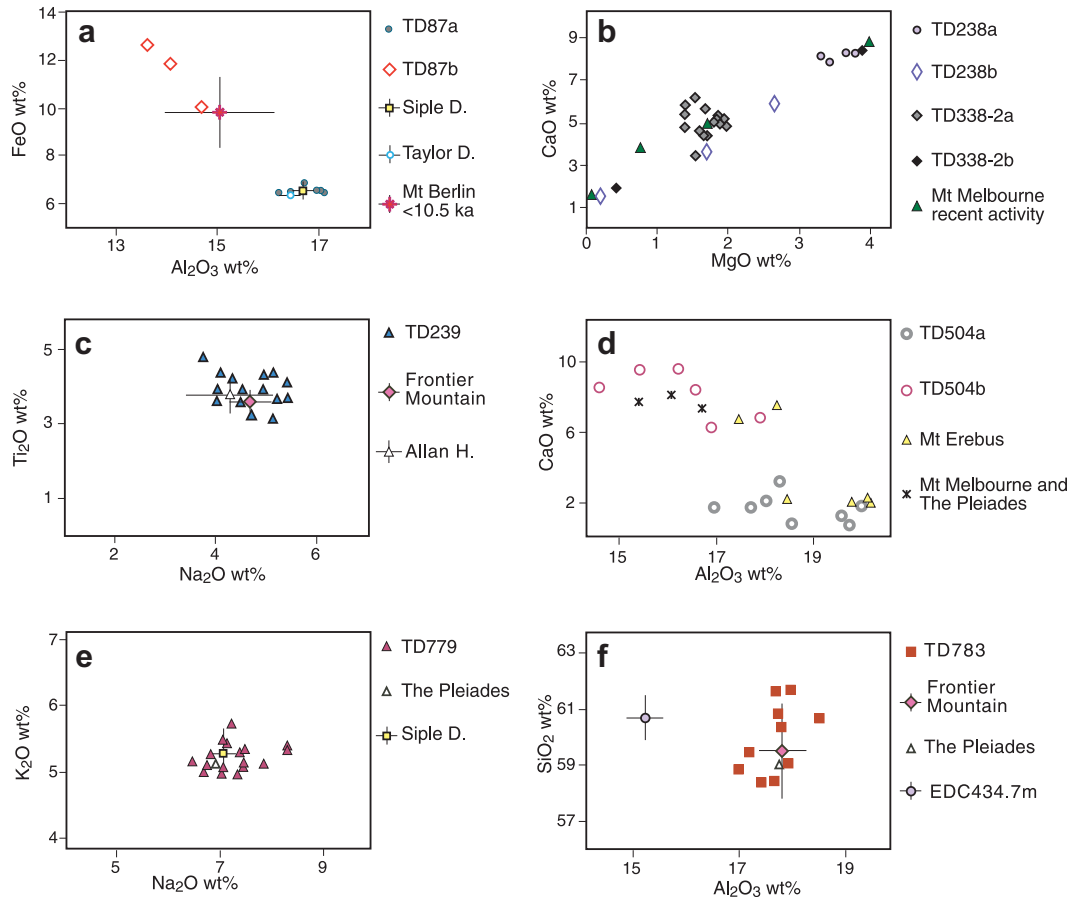
Fig. 5. Biplots of selected oxides (wt%) in TALDICE glass shards related to Antarctic sources compared with analyses of relevant volcanic samples taken from the literature (see references in the text). Error bars indicate one standard deviation.

the last 30 ka (Harpel et al., 2008). TD504a shows some geochemical similarities with Erebus tephras and may be the counterpart of one of the ash beds widely deposited on the flanks of the volcano after 15 ± 4 ka. Further experimental work, however, is needed to corroborate this attribution. The less differentiated (SiO_2 47–50 wt %) glass population TD504b is also compatible with Mount Erebus

geochemistry (Kyle et al., 1992). However, phonotephritic products are not recorded among the late Pleistocene to recent tephra products (Harpel et al., 2008) and according to the volcanic che-mostratigraphy reconstructed by Esser et al. (2004) this volcanic rock type belongs to an old (400–300 ka) phase of Erebus activity. Therefore, more probably TD504b is related to an eruption from
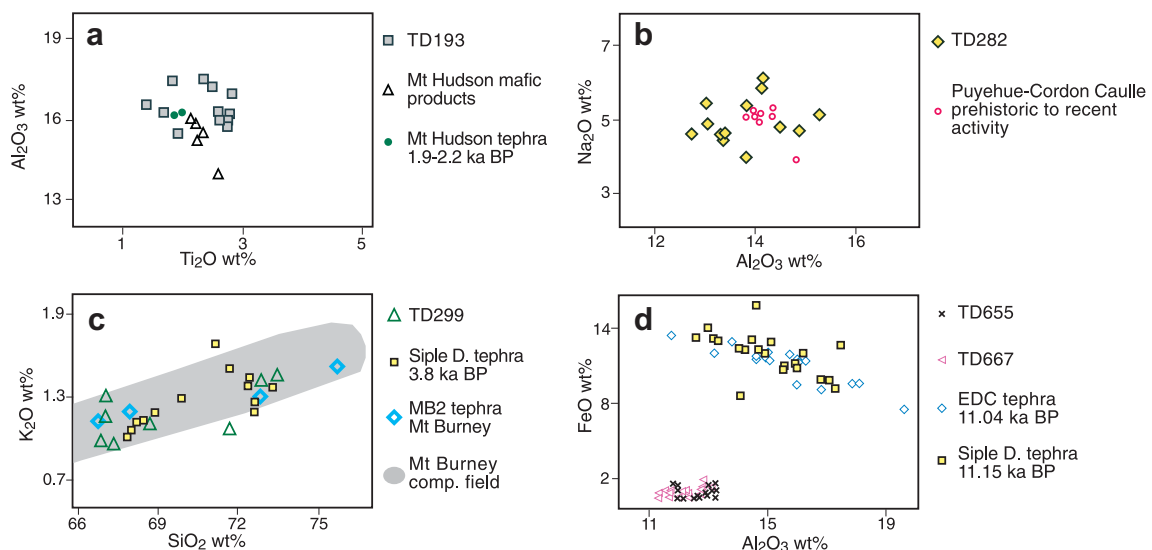
Fig. 6. Biplots of selected oxides (wt%) in TALDICE glass shards related to extra-Antarctic sources compared with analyses of relevant volcanic samples taken from the literature (see references in the text).
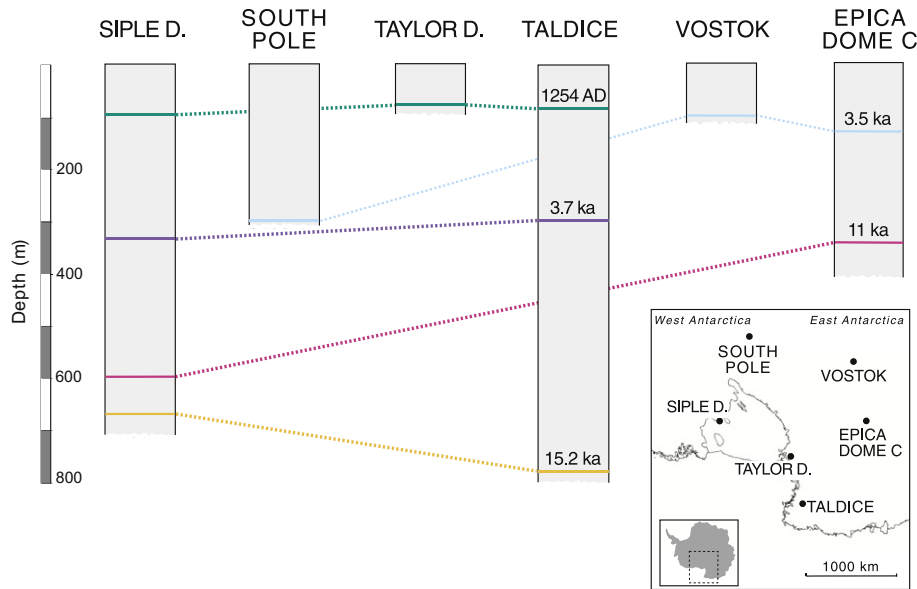
Fig. 7. Widespread isochronous tephra layers for the last 16 ka connecting ice cores from different sectors of the Antarctic ice sheet (location map of the study area and core sites is shown in the box).

volcanoes of the Melbourne Province, which occurred almost simultaneously to the explosive event that produced the phonolitic glass component within the same ice sample.

Visible tephra layers **TD681**, **TD720** and **TD741** are from ice levels dated 11.82 ± 0.13 ka BP, 13.01 ± 0.13 ka BP and 13.77 ± 0.13 ka BP, respectively, and were sourced from local volcanoes. Based on the $\delta^{18}O$ temperature-proxy record (Fig. 1), TD681 occurs at the start of the early Holocene while the older two samples fall within the Antarctic Cold Reversal (ACR), a short cooling episode well documented in Antarctic ice cores (Jouzel et al., 1995). These are indeed interesting stratigraphic positions for correlation purposes, if counterparts of these ash layers will be identified in other Antarctic climate records.

Sample **TD779** (15.19 ± 0.14 ka BP) falls ca six centuries before the Antarctic Isotopic Maximum (AIM) 1 event (Fig. 1). From the chemical point of view, this homogeneous tephra closely resembles The Pleiades rock composition (Fig. 5e). Moreover, it most likely equates to tephra SDMA9053 (15.3 ka) occurring in the Siple Dome ice core (Dunbar and Kurbatov, 2011). The two volcanic layers in fact have identical estimated ages and are also chemically very similar over the entire range of elements analysed (SC 0.95). We conclude that the two widely-spaced tephra horizons were deposited simultaneously during the same powerful explosive eruption from a Melbourne volcano. The layer forms a valuable stratigraphic horizon for secure correlation between East and West Antarctic climate records (Fig. 7).

The oldest tephra layer characterised in this investigation, **TD783** (15.37 ± 0.15 ka BP), lies within the climatic record in correspondence of a small isotopic peak preceding AIM1 (Fig. 1). It is trachytic in composition and is remarkably similar to rocks from The Pleiades volcanoes (Kyle, 1982). Its chemical features (Fig. 5f) closely match those of ZE-ZF tephra pair in the Frontier Mountain ice field (SC 0.97) that occurs stratigraphically below the counterpart for our sample TD239 (Fig. 10 of Curzio et al., 2008). Although no age data are available for the exposed tephra, it is most likely that the TALDICE and the blue ice layers correlate each other. This correlation, along with that one related to the 2.70-ka old tephra TD239 presented above, help date the Frontier Mountain series that was claimed to represent an ideal outcropping counterpart of TALDICE ice core (Curzio et al., 2008). It appears that more than half

of the estimated stratigraphic thickness of outcropping blue ice is younger than 15 ka. This chronological framework contradicts two terrestrial ages of meteorites trapped within the ice series (Folco et al., 2006) while it is consistent with the oxygen isotopic composition of Frontier Mountain ice samples (mean $\delta^{18}O$ value −36.0 ± 2.5‰) suggesting that a considerable part of the exposed blue ice formed under Holocene climatic conditions (mean $\delta^{18}O$ value −36.5 ± 0.8‰, see Fig. 1). Moreover, it is interesting to note that trachytic tephra TD783 has the same chronostratigraphic position of the EDC 434.7 m layer (15.34 ± 0.15 ka BP according to Lemieux-Dudon et al., 2010), also chemically classified as trachyte (Narcisi et al., 2005). However, the two layers are unrelated as they display different chemical signature (SC 0.79), TD783 being clearly similar to the Melbourne rock suite, the EPICA ash closely matching Mount Berlin products (Fig. 5f). This example emphasizes once more the importance of a multiple-criterion approach to avoid miscorrelation of tephra (e.g. Lowe, 2011). Age and stratigraphic data in fact are important in constraining compatible tephra link but careful comparison of geochemical data is vital to discriminate among seemingly similar layers.

4.2. Extra-Antarctic tephra layers

A large number of volcanic provinces surrounding Antarctica are potential parental volcanoes for the suite of TALDICE volcanic horizons characterised by fine grain size and sub-alkaline compositions. Thorough examination of tephra geochemical signatures and chronological constraints help limit sources. Products from the South Sandwich Islands, a very important source of ash in long ice cores drilled in the central East Antarctic Plateau (Narcisi et al., 2010b; and references therein), are characterised by very low K contents (Leat et al., 2003), those from South Shetland volcanoes are characterised by high Na contents (Smellie, 1990). None of these distinctive chemical features were detected in the glass fraction of the studied horizons, leading to discard both South Sandwich and South Shetland volcanoes. Rhyolitic products, somewhat similar to glass from TD341, TD655 and TD667 samples, occur also in West Antarctic volcanoes but they were erupted in Plio-Pleistocene (e.g. Shane and Froggatt, 1992), well before the time period considered in this work.

Both southern Andes and New Zealand volcanoes have been active ash-producers in the past 16,000 years (e.g. Lowe et al., 2008; Stern, 2008). Andes distal tephras were already identified at various places in Antarctica (e.g. Narcisi et al., 2010b; and references therein) while occurrence of New Zealand ash has only been tentatively suggested so far (Kurbatov et al., 2006). Within this work, we tested the occurrence and frequency of air mass trajectories capable of transporting volcanic ash to the Talos Dome site from the Andean volcanic regions and the Taupo Volcanic zone in New Zealand, respectively. We applied the HYSPLIT (HYbrid Single-Particle Lagrangian Integrated Trajectory) model (Draxler and Rolph, 2011), using the ECMWF Re-Analysis ERA-INTERIM data field as the input meteorological dataset. We calculated a set of 10-day back trajectories (TJ) for every day from 01/01/1990 to 31/12/2010 (total 7670), choosing different starting heights above Talos Dome (Fig. 8). For the Andean area, the analysis shows frequencies over 10% of the total calculated TJ and a single TJ path along the South polar clockwise atmospheric circulation, with a maximum occurrence between 8 and 10 km above Talos Dome. As regards New Zealand, maximum occurrence frequencies (8 km above the drilling site) represent only 1% of the calculated TJ dataset. Moreover, we identified two different paths, one passing over the Eastern South Pacific Ocean and connecting directly the volcanic area to Talos Dome, and the other one, more similar to the pathway from South America, following the typical atmospheric circulation encircling Antarctica. To sum up, the calculated TJ frequencies suggest that Andean volcanoes can represent a suitable source for tephra in the TALDICE core, while events of ash transport from New Zealand appear rare but still possible. Our analysis demonstrates that the clockwise circum-Antarctic atmospheric circulation can play a major role in the transport of particulate volcanic matter from volcanic centres to the Ross Sea region of the East Antarctic Plateau.

We shall now present the detected volcanic horizons and attempt to identify the provenance and to establish correlation between tephra records.

Sample **TD193** is trachybasaltic in composition (Table 3) and is assigned an age of 2.02 ka BP. Calc-alkaline mafic products were emitted by volcanoes in the southernmost part of the Andean Southern Volcanic Zone (Gutiérrez et al., 2005). In particular, the TALDICE tephra appears very similar in composition to products from Mount Hudson (ca 46°S, southern Chile), a volcano that has been frequently active during the Holocene (Haberle and Lumley, 1998; Naranjo and Stern, 1998). Among the known tephra deposits of Mount Hudson, we suggest that TD193 could be correlated with a distinctive tephra of mafic composition bracketed between uncalibrated radiocarbon ages 1910 ± 70 and 2235 ± 130 yr BP (Naranjo and Stern, 1998). This regionally significant Hudson tephra shows chemical similarities and radiochronological age overlapping with the TALDICE ice core tephra (Fig. 6a). Also glass geochemistry of **TD216** (2.35 ka BP) is similar to composition of the more evolved products of Mount Hudson (e.g. Kilian et al., 2003), however no silicic tephra of similar age has been recognised so far near the source (Naranjo and Stern, 1998).

Glass composition of tephra **TD282** (3.39 ka BP) falls within compositional field of Reclus volcano (ca 51°S, Andean Austral Volcanic Zone), however no significant Late Holocene eruptions are known from this volcano (Stern, 2008). Alternatively, the ice core tephra could be originated from an Andean volcano of Southern part the Southern Volcanic Zone. In particular, we found chemical affinities to products from Chile's Puyehue-Cordón Caulle volcanic complex (40.5°S) that erupted copious rhyodacite and rhyolite (Gerlach et al., 1988; Singer et al., 2008). Proximal volcanic stratigraphy shows a thick tephra sequence deposited between 10.5 and 1.1 ka BP and the prehistoric to recent products are chemically similar to TD282 (Fig. 6b). Tephra plumes from Puyehue-Cordón Caulle eruptions could have been blown vast distances, as was observed during the June–July 2011 eruption when volcanic ash entered into the polar vortex circulation encircling Antarctica, producing repeated flight disruption over South America, South Africa, Australia and New Zealand (Smithsonian Institution, 2012). In conclusion, this TALDICE tephra is most likely from Andean volcanic activity and a possible parent volcano may be Puyehue-Cordón Caulle, although no correlation with any specific tephra event can be proposed.

The invisible volcanic horizon **TD299** (3.68 ka BP) shows heterogeneous glass composition from dacite to rhyolite and relatively low potassium content (Table 3 and Fig. 6c). Based on consistent chemical signature (SC 0.94), and similar glass compositional trend (Fig. 6c) and estimated age, we propose that this tephra correlates with tephra sample SDMA2571 identified in the Siple Dome ice record at 3.8 ka BP (Kurbatov et al., 2006) (Fig. 7). Our tephra and the correlated Siple Dome sample could be related to activity of Mount Burney (ca 52°S), an Andean volcano of the Austral Volcanic Zone (Stern and Kilian, 1996). In particular, the late Holocene (3818–4711 cal years BP) MB_2 marker bed produced by Mount Burney and occurring in southernmost Patagonia (Stern, 2008) shows chemical characteristics (Fig. 6c) and radiometric age compatible with those of the ice core samples and its wide areal distribution southeast of the volcano is consistent with an ash transport towards East Antarctica by typical clockwise atmospheric circulation. We suggest that the TALDICE and Siple Dome ice core layers and the Mount Burney tephra could form a single well-dated time plane and, to our knowledge, this is the first notification of ash stratigraphic connection across Antarctica and South America regions. From the volcanological point of view, our finding emphasizes the extensive nature of this Mount Burney tephra and adds information relevant to revise previous estimates of the areal distribution and volume of the erupted products (Stern, 2008).

Fig. 8. Upper panel: principal 10-day back trajectory paths from Andean volcanic (blue line) and New Zealand (red lines) regions to Talos Dome. Lower panel: occurrence frequency for back trajectories starting at different heights and connecting the two source volcanic areas and Talos Dome (left *y* axis for Andes, right *y* axis for New Zealand). (For interpretation of the references to colour in this figure legend, the reader is referred to the web version of this article.)

Sample **TD341** is rhyolitic in composition and is assigned an age of 4.42 ka BP. Volcanic products with high silica content have been frequently erupted in the Austral and Southern Volcanic Zones of the Andes during the Holocene (Stern, 2008). The high K_2O content displayed by the studied sample (Table 3) is compatible with geochemistry of Aguilera volcano (50°S) that produced a sequence of Late Holocene tephras, one of which is dated to <4560 ^{14}C years BP (Stern, 2008). Unfortunately, a possible correlation between our sample and this Aguilera tephra cannot be tested because no chemical data are available. Alternatively, the TALDICE ash could be possibly derived from New Zealand volcanoes, where rhyolitic explosive eruptions repeatedly occurred during the Late Holocene (Gehrels et al., 2006). The age of the so-called Stent tephra (Unit Q) from Taupo (4240−4510 cal years BP) perfectly overlaps with the estimated age of TD341, however the two glass geochemistries are not fully consistent (SC 0.87). Therefore, source of TD341 remains uncertain.

Silicic samples **TD655** (11.20 ± 0.14 ka BP) and **TD667** (11.48 ± 0.13 ka BP) fall in the early Holocene (Fig. 1). Potential sources for these TALDICE tephras are both Andes and New Zealand volcanoes that erupted rhyolites in the early Holocene. The published Holocene tephrostratigraphy for the southernmost South America (Stern, 2008) does not include marker beds corresponding in terms of both chemistry and age to these Talos Dome samples. They could be related to modest unrecorded eruptions from Andean volcanoes, the ash of which has been rapidly transported to the Antarctic site by efficient circum-Antarctic westerly winds. Alternatively, the two studied samples could be derived from New Zealand volcanoes. Among regionally significant volcanic markers erupted in New Zealand (Lowe et al., 2008), Taupo rhyolitic tephras Poronui/C (ca 11,190 cal years BP) and Karapiti/B (ca 11,410 cal years BP) fall in the Early Holocene warming period and are precisely coeval with ice core volcanic horizons. However, chemical comparison between the New Zealand tephra couplet and the TALDICE samples do not fully agree (SC 0.84 and 0.87, respectively), maybe due to inaccuracies inherent in the analysis of very small and irregularly shaped glass shards in the ice. Imperfect chemical matching leaves this hypothetical widespread correlation unproved but work is in progress aimed at re-sampling the ice core volcanic horizons for electron probe microanalysis on polished mounts. We also investigated potential stratigraphic correlations across Antarctica, based on comparison of tephra composition and age. Although these TALDICE horizons are expected to occur at other sites of the Antarctic ice sheet, we found that they are not related to any ice core tephra identified so far. Both the EDC tephra layer occurring at 339.5 m depth (Narcisi et al., 2005) and dated at 11.04 ± 0.14 ka BP (Lemieux-Dudon et al., 2010) and the 11.15-ka ash horizon detected in the Siple Dome A core (Kurbatov et al., 2006; Dunbar and Kurbatov, 2011) are geochemically dissimilar and unrelated to the studied samples (Fig. 6d). Interestingly, here we note that the above-mentioned EDC and Siple Dome layers correlate each other. In fact, glass chemistries of the two tephras are highly comparable (SC 0.94) and also display coincident variability along a fractionation trend (Fig. 6d). This new tephra correlation is further confirmed by the fact that the estimated age of the ice enclosing these layers is strikingly similar. Given its geochemical signature, this englacial ash very likely originates from a volcano outside Antarctica. It could be related to Mount Hudson, Chilean Andes (Kurbatov et al., 2006) or more probably to South Sandwich volcanoes, South Atlantic Ocean (Narcisi et al., 2005). Regardless of source, we conclude that the tephra layers in the two widely separated ice cores (ca 1800 km) are related to the same eruption and therefore form an important isochronous bed for precise comparison of East and West ice sheet climatic records (Fig. 7).

5. Significance of the presented findings and conclusions

We have detected traces of 26 distinct eruptions in the TALDICE core section covering the last deglaciation and the Holocene. The studied ice sequence appears dominated by Antarctic volcanic sources that produced two thirds of the identified tephra layers. The majority of Antarctic tephras geochemically matches products from the recent Melbourne sequence, confirming the potential of our ice core to provide information on stratigraphy and the tempo of explosive volcanism in northern Victoria Land (Narcisi et al., 2010a). The volcanic record of Antarctic derivation includes also two peculiar tephras, one probably derived from a Marie Byrd Land volcano and the other maybe from Mount Erebus. Our studies also point out the significant presence within the TALDICE record of airborne volcanic material sourced in volcanic provinces located outside the Antarctic continent. These findings provide palae-oatmospheric hints complementary to results from studies of continental dust in the ice core (e.g. Delmonte et al., 2010). In particular, occurrence at Talos Dome of volcanic ash from South America suggests that, similarly to central East Antarctica, also this peripheral site of the East Antarctic ice sheet was involved in incursions of air masses driven by the typical westerly circumpolar circulation. A further ramification is that we provide evidence for extended deposition of airborne products of known Andean eruptions as well as for occurrence of explosive events yet unrecognised in proximal localities. Such consequences highlight the importance of the study of distal tephra in volcanology.

Most importantly, this study brings significant stratigraphic implications. A few TALDICE layers have been successfully correlated with tephras found in other records of the Antarctic region. The network of correlated sites includes also Dome C (Fig. 7) that we securely linked to the Siple Dome ice record through the 11-ka tephra. Taken all together, the presented findings significantly extend the previous Antarctic tephrostratigraphic framework (Narcisi et al., 2005) to the Ross Sea sector and further away to the West Antarctic ice sheet (Fig. 7). East and West Antarctic ice climatic sequences are now tied at multiple depths. As some studied layers lie in critical stratigraphic positions within the ice core climate record (Fig. 1), the proposed tephra linkages could be fruitfully used in future studies addressing the lead−lag relationship on short timescales of different climate archives.

Some far-travelled tephras found in the Talos Dome core appear to be extensively dispersed not only in the Antarctic ice sheet but also outside the Antarctic continent, as is the case of the late Holocene tephra probably related to Mount Burney, which occurs in continental deposits of Patagonia. It is likely that the recognised continental-scale tephra markers could be present also in other archives, as the East Antarctic ice cores facing the Atlantic Ocean sector and the South Atlantic marine sediment cores. Other tephras have been identified so far only at TALDICE, however they are distinguishable from others for their chemical characteristics and thus have the potential of being recognised at other sites when new ice cores will become available and the enclosed tephra layers analysed. Finally, along with successful correlations, we illustrated examples of uncorrelated tephras and pointed out the need of combining geochemical and chronological evidence to avoid erroneous correlations.

In conclusion, the highly resolved tephra record at TALDICE contributes significantly to the construction of the Antarctic tephra time-stratigraphic framework. Future work extending the tephra record to the last glacial period would be of high interest, given the prospects for precisely aligning different cores and then testing synchroneity of the related climatic events. Moreover, marine and terrestrial sediments from circumpolar regions could be inspected for the search of the widespread tephras from extra-Antarctic

sources detected in the present study. In this respect, the related tephra-based correlations could be helpful to circumvent the chronological issues inherent in comparing records from different realms.

Acknowledgements

References

Albani, S., Delmonte, B., Maggi, V., Baroni, C., Petit, J.-R., Stenni, B., Mazzola, C., Frezzotti, M., 2012. Interpreting last glacial to Holocene dust changes at Talos Dome (East Antarctica): implications for atmospheric variations from regional to hemispheric scales. Climate of the Past 8, 741–750.

Borchardt, G.A., Aruscavage, P.J., Millard, H.T.J., 1972. Correlation of the Bishop ash, a Pleistocene marker bed, using instrumental neutron activation analysis. Journal of Sedimentary Petrology 42 (2), 301–306.

Buiron, D., Chappellaz, J., Stenni, B., Frezzotti, M., Baumgartner, M., Capron, E., Landais, A., Lemieux-Dudon, B., Masson-Delmotte, V., Montagnat, M., Parrenin, F., Schilt, A., 2011. TALDICE-1 age scale of the Talos Dome deep ice core, East Antarctica. Climate of the Past 7, 1–16.

Curzio, P., Folco, L., Laurenzi, M.A., Mellini, M., Zeoli, A., 2008. A tephra chronostratigraphic framework for the Frontier Mountain blue-ice field (northern Victoria Land, Antarctica). Quaternary Science Reviews 27, 602–620.

Davies, S.M., Wastegård, S., Abbott, P.M., Barbante, C., Bigler, M., Johnsen, S.J., Rasmussen, T.L., Steffensen, J.P., Svensson, A., 2010. Tracing volcanic events in the NGRIP ice-core and synchronising North Atlantic marine records during the last glacial period. Earth and Planetary Science Letters 294, 69–79.

Delmonte, B., Petit, J.R., Maggi, V., 2002. Glacial to Holocene implications of the new 27000-year dust record from the EPICA Dome C (East Antarctica) ice core. Climate Dynamics 18, 647–660.

Delmonte, B., Baroni, C., Andersson, P.S., Schoberg, H., Hansson, M., Aciego, S., Petit, J.-R., Albani, S., Mazzola, C., Maggi, V., Frezzotti, M., 2010. Aeolian dust in the Talos Dome ice core (East Antarctica, Pacific/Ross Sea sector): Victoria Land versus remote sources over the last two climate cycles. Journal of Quaternary Science 25, 1327–1337.

Draxler, R.R., Rolph, G.D., 2011. HYSPLIT (HYbrid Single-Particle Lagrangian Integrated Trajectory). Model access via NOAA ARL READY Website. NOAA Air Resources Laboratory, Silver Spring, MD. http://ready.arl.noaa.gov/HYSPLIT.php.

Dunbar, N.W., Kurbatov, A.V., 2011. Tephrochronology of the Siple Dome ice core, West Antarctica: correlations and sources. Quaternary Science Reviews 30, 1602–1614.

Dunbar, N.W., Zielinski, G.A., Voisins, D.T., 2003. Tephra layers in the Siple Dome and Taylor Dome ice cores, Antarctica: sources and correlations. Journal of Geophysical Research 108, 2374. http://dx.doi.org/10.1029/2002JB002056.

Dunbar, N.W., McIntosh, W.C., Esser, R.P., 2008. Physical setting and tephrochronology of the summit caldera ice record at Mount Moulton, West Antarctica. Geological Society of America Bulletin 120, 796–812.

Dunbar, N.W., Kurbatov, A.V., Koffman, B.G., Kreutz, K.J., 2010. Tephra Record of Local and Distal Volcanism in the WAIS Divide Ice Core. 2010 WAIS Divide Science Meeting September 30–October 1, La Jolla, CA.

Esser, R.P., Kyle, P.R., McIntosh, W.C., 2004. $^{40}Ar/^{39}Ar$ dating of the eruptive history of Mount Erebus, Antarctica: volcano evolution. Bulletin of Volcanology 66, 671–686.

Fiacco, R.J., Palais, J.M., Germani, M.S., Zielinski, G.A., Mayewski, P.A., 1993. Characteristics and possible source of a 1479 A.D. volcanic ash layer in a Greenland ice core. Quaternary Research 39, 267–273.

Folco, L., Welten, K.C., Jull, A.J.T., Nishiizumi, K., Zeoli, A., 2006. Meteorites constrain the age of Antarctic ice at the Frontier Mountain blue-ice field (northern Victoria Land). Earth and Planetary Science Letters 248, 209–216.

Frezzotti, M., Urbini, S., Proposito, M., Scarchilli, C., Gandolfi, S., 2007. Spatial and temporal variability of surface mass balance near Talos Dome, East Antarctica. Journal of Geophysical Research 112, F02032. http://dx.doi.org/10.1029/2006JF000638.

Froggatt, P.C., 1992. Standardization of the chemical analysis of tephra deposits. Report of the ICCT working group. Quaternary International 13/14, 93–96.

Gehrels, M.J., Lowe, D.J., Hazell, Z.J., Newnham, R.M., 2006. A continuous 5300-yr Holocene cryptotephrostratigraphic record from northern New Zealand and implications for tephrochronology and volcanic assessment. The Holocene 16, 173–187.

Gerlach, D.C., Frey, F.A., Moreno, H., Lopez-Escobar, L., 1988. Recent volcanism in the Puyehue-Cordon Caulle region, southern Andes, Chile (40.5°S): petrogenesis of evolved lavas. Journal of Petrology 29, 333–382.

Gutiérrez, F., Gioncada, A., González Ferran, O., Lahsen, A., Mazzuoli, R., 2005. The Hudson Volcano and surrounding monogenetic centres (Chilean Patagonia): an example of volcanism associated with ridge-trench collision environment. Journal of Volcanology and Geothermal Research 145, 207–233.

Haberle, S.G., Lumley, S.H., 1998. Age and origin of tephras recorded in postglacial lake sediments to the west of the Southern Andes, 44°S to 47°S. Journal of Volcanology and Geothermal Research 84, 239–256.

Harpel, C.J., Kyle, P.R., Dunbar, N.W., 2008. Englacial tephrostratigraphy of Erebus volcano, Antarctica. Journal of Volcanology and Geothermal Research 177, 549–568.

Hillenbrand, C.-D., Moreton, S.G., Caburlotto, A., Pudsey, C.J., Lucchi, R.G., Smellie, J.L., Benetti, S., Grobe, H., Hunt, J.B., Larter, R.D., 2008. Volcanic time-markers for Marine Isotopic Stages 6 and 5 in Southern Ocean sediments and Antarctic ice cores: implications for tephra correlations between palaeoclimatic records. Quaternary Science Reviews 27, 518–540.

Jochum, K.P., Stoll, B., Herwig, K., Willbold, M., Hofmann, A.W., Amini, M., Aarburg, S., Abouchami, W., Hellebrand, E., Mocek, B., Raczek, I., Stracke, A., Alard, O., Bouman, C., Becker, S., Ducking, M., Brätz, H., Klemd, R., de Bruin, D., Canil, D., Cornell, D., de Hoog, C.J., Dalpé, C., Danyushevsky, L., Eisenhauer, A., Gao, Y., Snow, J.E., Groschopf, N., Günther, D., Latkoczy, C., Guillong, M., Hauri, E.H., Höfer, H.E., Lahaye, Y., Horz, K., Jacob, D.E., Kasemann, S.A., Kent, A.J.R., Ludwig, T., Zack, T., Mason, P.R.D., Meixner, A., Rosner, M., Misawa, K., Nash, B.P., Pfänder, J., Premo, W.R., Sun, W.D., Tiepolo, M., Vannucci, R., Vennemann, T., Wayne, D., Woodhead, J.D., 2006. MPI-DING reference glasses for in situ microanalysis: new reference values for element concentrations and isotope ratios. Geochemistry Geophysics Geosystems 7, Q02008. http://dx.doi.org/10.1029/2005GC001060.

Jouzel, J., Vaikmae, R., Petit, J.R., Martin, M., Duclos, Y., Stievenard, M., Lorius, C., Toots, M., Mélières, M.A., Burckle, L.H., Barkov, N.I., Kotlyakov, V.M., 1995. The two-step shape and timing of the last deglaciation in Antarctica. Climate Dynamics 11, 151–161.

Jouzel, J., Masson-Delmotte, V., Cattani, O., Dreyfus, G., Falourd, S., Hoffmann, G., Minster, B., Nouet, J., Barnola, J.M., Chappellaz, J., Fischer, H., Gallet, J.C., Johnsen, S., Leuenberger, M., Loulergue, L., Luethi, D., Oerter, H., Parrenin, F., Raisbeck, G., Raynaud, D., Schilt, A., Schwander, J., Selmo, E., Souchez, R., Spahni, R., Stauffer, B., Steffensen, J.P., Stenni, B., Stocker, T.F., Tison, J.L., Werner, M., Wolff, E.W., 2007. Orbital and millennial Antarctic climate variability over the past 800,000 years. Science 317, 793–796.

Kilian, R., Hohner, M., Biester, H., Wallrabe-Adams, H.J., Stern, C.R., 2003. Holocene peat and lake sediment tephra record from the southernmost Chilean Andes (53–55°S). Revista Geológica de Chile 30, 23–37.

Kurbatov, A.V., Zielinski, G.A., Dunbar, N.W., Mayewski, P.A., Meyerson, E.A., Sneed, S.B., Taylor, K.C., 2006. A 12,000 year record of explosive volcanism in the Siple Dome ice core, West Antarctica. Journal of Geophysical Research 111, D12307. http://dx.doi.org/10.1029/2005JD006072.

Kyle, P.R., 1982. Volcanic geology of the Pleiades, Northern Victoria Land, Antarctica. In: Craddock, C. (Ed.), Antarctic Geoscience. The University of Wisconsin Press, Madison, pp. 747–754.

Kyle, P.R., Moore, J.A., Thirlwall, M.F., 1992. Petrologic evolution of anorthoclase phonolite lavas at Mount Erebus, Ross Island, Antarctica. Journal of Petrology 33, 849–875.

Le Bas, M.J., Le Maitre, R.W., Streckeisen, A., Zanettin, B., 1986. A chemical classification of volcanic rocks based on the total alkali-silica diagram. Journal of Petrology 27, 745–750.

Leat, P.T., Smellie, J.L., Millar, I.L., Larter, R.D., 2003. Magmatism in the South Sandwich arc. In: Geological Society of London Special Publications, vol. 219, pp. 285–313.

Lemieux-Dudon, B., Blayo, E., Petit, J.-R., Waelbroeck, C., Svensson, A., Ritz, C., Barnola, J.-M., Narcisi, B., Parrenin, F., 2010. Consistent dating for Antarctic and Greenland ice cores. Quaternary Science Reviews 29, 8–20.

Loulergue, L., Schilt, A., Spahni, R., Masson-Delmotte, V., Blunier, T., Lemieux, B., Barnola, J.-M., Raynaud, D., Stocker, T.F., Chappellaz, J., 2008. Orbital and millennial-scale features of atmospheric CH_4 over the past 800,000 years. Nature 453, 383–386.

Lowe, D.J., 2011. Tephrochronology and its application: a review. Quaternary Geochronology 6, 107–153.

Lowe, D.J., Shane, P.A.R., Alloway, B.V., Newnham, R.M., 2008. Fingerprints and age models for widespread New Zealand tephra marker beds erupted since 30,000 years ago: a framework for NZ-INTIMATE. Quaternary Science Reviews 27, 95–126.

Masson-Delmotte, V., Buiron, D., Ekaykin, A., Frezzotti, M., Gallée, H., Jouzel, J., Krinner, G., Landais, A., Motoyama, H., Oerter, H., Pol, K., Pollard, D., Ritz, C., Schlosser, E., Sime, L.C., Sodemann, H., Stenni, B., Uemura, R., Vimeux, F., 2011.

A comparison of the present and last interglacial periods in six Antarctic ice cores. Climate of the Past 7, 397–423.

Morgan, G.B.V.I., London, D., 2005. Effect of current density on the electron microprobe analysis of alkali aluminosilicate glasses. American Mineralogist 90, 1131–1138.

Naranjo, J.A., Stern, C.R., 1998. Holocene explosive activity of Hudson volcano, southern Andes. Bulletin of Volcanology 59, 291–306.

Narcisi, B., Proposito, M., Frezzotti, M., 2001. Ice record of a 13th century explosive volcanic eruption in northern Victoria Land, East Antarctica. Antarctic Science 13, 174–181.

Narcisi, B., Petit, J.R., Delmonte, B., Basile-Doelsch, I., Maggi, V., 2005. Characteristics and sources of tephra layers in the EPICA-Dome C ice record (East Antarctica): implications for past atmospheric circulation and ice core stratigraphic correlations. Earth and Planetary Science Letters 239, 253–265.

Narcisi, B., Petit, J.R., Tiepolo, M., 2006. A volcanic marker (92 ka) for dating deep east Antarctic ice cores. Quaternary Science Reviews 25, 2682–2687.

Narcisi, B., Petit, J.R., Chappellaz, J., 2010a. A 70 ka record of explosive eruptions from the TALDICE ice core (Talos Dome, East Antarctic plateau). Journal of Quaternary Science 25, 844–849.

Narcisi, B., Petit, J.R., Delmonte, B., 2010b. Extended East Antarctic ice core tephrostratigraphy. Quaternary Science Reviews 29, 21–27.

Nishio, F., Katsushima, T., Ohmae, H., 1985. Volcanic ash layers in bare ice areas near the Yamato Mountains, Dronning Maud Land and the Allan Hills, Victoria Land, Antarctica. Annals of Glaciology 7, 34–41.

Palais, J.M., Kyle, P.R., Mosley-Thompson, E., Thomas, E., 1987. Correlation of a 3,200 year old tephra in ice cores from Vostok and South Pole stations, Antarctica. Geophysical Research Letters 14 (8), 804–807.

Rickwood, P.C., 1989. Boundary lines within petrologic diagrams which uses oxides of major and minor elements. Lithos 22, 247–263.

Schilt, A., Baumgartner, M., Schwander, J., Buiron, D., Capron, E., Chappellaz, J., Loulergue, L., Schüpbach, S., Spahni, R., Fischer, H., Stocker, T.F., 2010. Atmospheric nitrous oxide during the last 140,000 years. Earth and Planetary Science Letters 300, 33–43.

Severi, M., Udisti, R., Becagli, S., Stenni, B., Traversi, R., 2012. Volcanic synchronisation of the EPICA-DC and TALDICE ice cores for the last 42 kyr BP. Climate of the Past 8, 509–517.

Shane, P.A.R., Froggatt, P.C., 1992. Composition of widespread volcanic glass in deep-sea sediments of the Southern Pacific Ocean: an Antarctic source inferred. Bulletin of Volcanology 54, 595–601.

Singer, B.S., Jicha, B.R., Harper, M.A., Naranjo, J.A., Lara, L.E., Moreno-Roa, H., 2008. Eruptive history, geochronology, and magmatic evolution of the Puyehue-Cordón Caulle volcanic complex, Chile. Geological Society of America Bulletin 120, 599–618.

Smellie, J.L., 1990. Graham Land and South Shetland islands − summary. In: LeMasurier, W.E., Thomson, J.W. (Eds.), Volcanoes of the Antarctic Plate and Southern Oceans. Antarctic Research Series, vol. 48, pp. 303–312.

Smellie, J.L., 1999. The upper Cenozoic tephra record in the south polar region: a review. Global and Planetary Change 21, 51–70.

Smithsonian Institution, 2012. Puyehue-Cordón Caulle. Bulletin of the Global Volcanism Network 37 (3), 8–13.

Stenni, B., Buiron, D., Frezzotti, M., Albani, S., Barbante, C., Bard, E., Barnola, J.M., Baroni, M., Baumgartner, M., Bonazza, M., Capron, E., Castellano, E., Chappellaz, J., Delmonte, B., Falourd, S., Genoni, L., Iacumin, P., Jouzel, J., Kipfstuhl, S., Landais, A., Lemieux-Dudon, B., Maggi, V., Masson-Delmotte, V., Mazzola, C., Minster, B., Montagnat, M., Mulvaney, R., Narcisi, B., Oerter, H., Parrenin, F., Petit, J.R., Ritz, C., Scarchilli, C., Schilt, A., Schüpbach, S., Schwander, J., Selmo, E., Severi, M., Stocker, T.F., Udisti, R., 2011. Expression of the bipolar seesaw in Antarctic climate records during the last deglaciation. Nature Geoscience 4, 46–49.

Stern, C.R., 2008. Holocene tephrochronology record of large explosive eruptions in the southernmost Patagonian Andes. Bulletin of Volcanology 70, 435–454.

Stern, C.R., Kilian, R., 1996. Role of the subducted slab, mantle wedge and continental crust in the generation of adakites from the Andean Austral Volcanic Zone. Contributions to Mineralogy and Petrology 123, 263–281.

Wilch, T.I., McIntosh, W.C., Dunbar, N.W., 1999. Late Quaternary volcanic activity in Marie Byrd Land: potential ^{40}Ar/^{39}Ar-dated time horizons in West Antarctic ice and marine cores. Geological Society of America Bulletin 111 (10), 1563–1580.

Wörner, G., 1999. Lithospheric dynamics and mantle sources of alkaline magmatism of the Cenozoic West Antarctic rift system. Global and Planetary Change 23, 61–77.

Wörner, G., Viereck, L., Hertogen, J., Niephaus, H., 1989. The Mt. Melbourne volcanic field (Victoria Land, Antarctica) II. Geochemistry and magma genesis. Geologisches Jahrbuch E38, 395–433.